Journal of Physics: Conference Series

PAPER • **OPEN ACCESS**

Numerical analysis of the flow in the model of a venous valve: normal and surgical corrected

To cite this article: Y A Gataulin *et al* 2021 *J. Phys.: Conf. Ser.* **2103** 012207

Numerical analysis of the flow in the model of a venous valve: normal and surgical corrected

Y A Gataulin[1*,2], A D Yukhnev[1,2] and D A Rosukhovskiy[2]

[1] Peter the Great St. Petersburg Polytechnic University, 29 Politechnicheskaya Street, St. Petersburg, 195251, Russia
[2] Institute of Experimental Medicine, 12 Acad. Pavlov Street, St. Petersburg, 197376, Russia

[*]e-mail: yakov_gataulin@mail.ru

Abstract. The present study aimed to modeling of surgically corrected venous valve. The Arbitrary Lagrangian-Eulerian (ALE) method was used to model the blood–leaflet interactions. The contact process between leaflets was evaluated using a frictionless contact method. The results of the numerical study of the flow in the venous valve after extravasal correction was compared with the results for the normal venous valve.

1. Introduction

Venous hydrodynamics is of particular theoretical and practical interest due to weak research (in comparison with arterial) and severity of venous diseases. One of diseases is chronic venous incompetence – a pathology that occurs as a result of violations of the venous outflow in the lower extremities. It is one of the most common diseases of the vascular venous system. Underestimation of the severity of the disease leads to serious consequences: inflammation, bleeding, thrombus formation, trophic ulcers. Numerical modeling is a convenient tool to simulate venous valve in normal or surgically corrected state.

Buxton et al. [1] employed a spring lattice model to illustrate the basic mechanics of vein valves. They investigated the dynamics of the valve opening area, and captured the unidirectional nature of the blood flow in venous valve. Owing to a few reports on the mechanical properties, limited studies have explored venous valve modeling, particularly for the pathological cases with insufficient biological knowledge. Of the existing numerical studies, only Soifer et al. [2] studied the effects of stiffened venous valves on the neighboring valve using the arbitrary Lagrange–Eulerian (ALE) method. Simão et al. [3] and Ariane et al. [4] modeled interaction between the thrombus agglomeration and the vein, studied the clotting dynamics and its effect on the reverse flow. Chen et al. [5] studied the helical flow induced by the relative positions of the valves and its corresponding effects on the stagnation zones. These studies are the essential step in studying the pathological vein valve, and they provided useful information on valve hemodynamics and improved the relevant understandings. Liu et al [6] studied the effect of venous valve lesion on the valve biomechanics. Four valve lesions induced by the abnormal elasticity variation were considered for the diseased valve: fibrosis, atrophy, incomplete fibrosis, and incomplete atrophy.

Previously in our study [7] a two-dimensional computational model of the incompetent popliteal venous valve was constructed and the effect of the gap width between the valve leaflets on the valve reverse flow (reflux) was investigated. Further [8] leaflet elasticity effect on flow structure was investigated based on that model. Numerical results had a good qualitative agreement with clinical ultrasound data on the position and size of the stagnant zone behind the leaflet. In the last our study [9] the model of a normal popliteal venous valve was constructed and the results of a numerical study of the flow with different leaflet elasticity were presented. Valve was under resting conditions and the focus was on the analysis of velocity field and stagnant region. Meanwhile, the above mentioned and most of other studies consider the normal and diseased venous valves. For the first time effect of surgical correction of incompetence venous valve is investigated.

The purpose of the work is to study the velocity field and stagnant zones in the model of normal venous valve and venous valve after extravasal correction.

2. Extravasal correction of chronic venous incompetence

A variety of venous valvular correction methods are known and they are still under permanent development [10]. One of the surgery for chronic venous incompetence of the lower limb is the extravasal correction. This method lies in vein narrowing in the valve area, which provides the closing of the leaflets and the correction of the valve function. There are different devices for extravasal correction of the lower extremities: muffs from autovein, artificial muffs, fascial paravasual structures, lavsan skeleton spirals, different alloys displaying shape memory effect and etc.

Using the extravasal correction method requires a vein narrowing by 1/3 – 1/4 of initial diameter of the valve area. With the help of numerical simulation, it is possible to obtain a fairly large amount of information about the flow in the venous valve, which can serve as a basis for improving the methods of venous valvular correction.

In our work the model of extravasal corrected popliteal venous valve with shortened leaflets of normal elasticity was constructed and studied.

3. Geometry models

The two-dimensional symmetry model of normal vein valve was constructed according to the characteristic dimensions of a popliteal vein based on clinical measurements [2], as illustrated in Fig.1. The normal vein model included a bileaflet valve, venous wall and sinus pockets. The vein radius R is 5 mm. The valve leaflet was semilunar shaped. The leaflet thickness and length (L) were 0.4 and 10 mm, respectively.

Vein model after extravasal correction had narrowing by 1/3 of radius (from 5 to 3.3 mm) at length of 5 cm and deleted sinus pockets. The leaflet thickness and length were 0.4 and 5 mm, respectively.

4. Boundary conditions and material properties

Boundary conditions and material properties according to clinical data were set identical for both studied models – normal valve and the one after extravasal correction. A uniform velocity profile and a variation in the bulk velocity over the cycle time taken from Soifer [2], were imposed at the inlet boundary (Fig. 2). The cycle period was T = 1.7 s. The velocity increase phase was 0.23T. The maximum bulk velocity is $V_{b\ max}$ = 0.07 m/s. Constant pressure was set at the outlet boundary. A rheological Newtonian model with density ρ_f = 1060 kg/m^3 and viscosity μ_f = 0.004 Pa·s was implemented. The flow was laminar with maximum Reynolds number $\mathrm{Re} = \rho_f R V_{b\max} / \mu_f = 90$ and Womersley number $Wo = R\sqrt{2\pi\rho_f / \left(T\mu_f\right)} \approx 5$. The approximation of rigid walls was used as their displacements are insignificant for the popliteal vein. The valve leaflets were assumed to be isotropic, linear elastic with density ρ_s =1200 kg/m^3, Poisson ratio ν_s = 0.45 and elastic modulus E = 0.2 MPa [2].

Figure 1. Venous valve models: normal valve (a) and incompetent valve after extravasal correction (b)

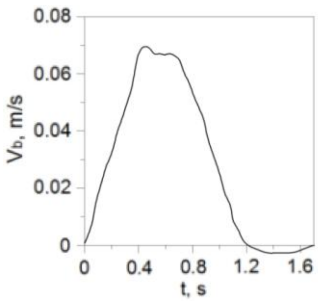

Figure 2. Variation in the bulk velocity during the cycle (for both models)

5. Mathematical model

In this study, ANSYS Fluent and Mechanical solvers were used for the fluid and structure modeling, respectively.

The governing equations are formulated using the Arbitrary Lagrangian-Eulerian (ALE) approach for modeling unsteady, incompressible fluid flow on a deforming mesh. In the ALE formulation, the continuity equation is written as

$$\nabla u_i = 0,$$

where $\boldsymbol{u}$ is the fluid velocity. For mesh velocity $\boldsymbol{u_m}$, a convective term $(u_j - u_{m\,j})$ is introduced, such that that the momentum equation in ALE formulation may be given

$$\frac{\partial u_i}{\partial t} + (u_j - u_{m\,j})\frac{\partial u_i}{\partial x_j} = -\frac{1}{\rho_f}\frac{\partial p}{\partial x_i} + \frac{1}{\rho_f}\frac{\partial}{\partial x_j}\left(\mu_f \frac{\partial u_i}{\partial x_j}\right), \quad i, j = 1,2$$

where p is the pressure and μ_f is the fluid dynamic viscosity.

The structure motion is described by the Lagrangian formulation. Solid with density ρ_s has the displacement $\boldsymbol{d_s}$ which is given by

$$\rho_s \frac{\partial^2 d_{s,i}}{\partial t^2} = \left(\nabla \cdot \left(S \cdot F^T\right)\right)_i + \rho_s f_{b,i}, \ i=1,2$$

where $\boldsymbol{f_b}$ is the body force and F is the deformation gradient tensor given by

$$F = I + \nabla d_s^T ,$$

where I is the identity and S is the Piola-Kirchoff stress tensor.

The Green-Lagrangian strain tensor G given by

$$G = \frac{\left(F^T F - I\right)}{2}$$

is related to S by the following relation:

$$S = 2\mu_s G + \lambda_s tr(G) I ,$$

where tr is the tensor trace and λ_s and μ_s are elastic material Lame constants. In ANSYS Structural, the elastic modulus E and the Poisson ratio v_s are specified as inputs and are related to λ_s and μ_s as

$$\lambda_s = \frac{E v_s}{(1+v_s)(1-2v_s)}, \ \mu_s = \frac{E}{2(1+v_s)}.$$

At the interface Γ, the following conditions were satisfied:

$$\boldsymbol{d}_s^\Gamma = \boldsymbol{d}_f^\Gamma, \ \boldsymbol{u}_s^\Gamma = \boldsymbol{u}_f^\Gamma, \ \boldsymbol{T}_s^\Gamma = -\boldsymbol{T}_f^\Gamma ,$$

where $\boldsymbol{T}^\Gamma$ is the traction force at the interface, which is the sum of the pressure and viscous forces.

6. Contact detection

Choosing the appropriate contact type depending on the type of solving problem is impotent task. There are several contact types, implemented in Ansys Mechanical; such as Bonded, Frictionless, Rough, Frictional, No Separation. All this contact types were tested for venous valve modeling. Testing computations showed that frictionless contact type was more physically adequate because of sliding like in the real valve (coaptation of leaflets). Besides this contact type is more robust due to weak spring stabilization. The frictionless contact type was chosen for basic computations.

Contact and target regions in our study were neighboring surfaces belonging to leaflet body and artificial body (Fig. 3). The last one modeled leaflet symmetric to the actual and had parallelepiped shape. Small gap of 0.1 mm between the artificial face and the symmetry face was preserved to prevent the fluid mesh collapse.

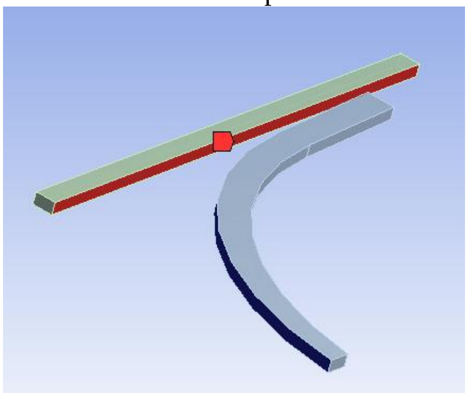

Figure 3. Contact (red) and target (blue) regions

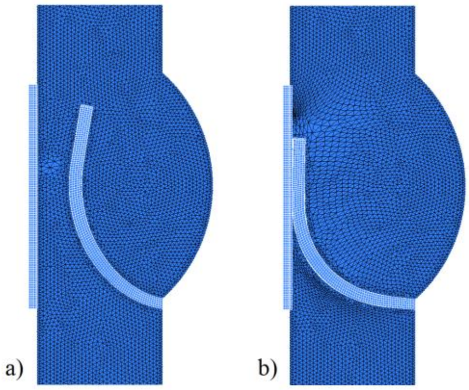

Figure 4. Computational meshes for normal valve in the opening (a) and closed (b) phase

7. Computational aspects

As the structure moves inside the fluid domain, fluid mesh deforms consequently (Fig. 4). In this study, the smoothing and remeshing mesh update methods were used. The computational domain was discretized using unstructured triangular mesh. Mesh around the leaflet was refined. Either the mesh size or the time step size was based on the considerations of mesh and time step sensitivity. The structural parts were discretized with a mesh of 5250 elements, 2750 of them comprised the leaflet. The flow domain was discretized with a mesh of approximately 185,000 elements. Time discretization of 0.01 s was used. In closed phase (when contact detection) time step was reduced to 0.001 s.

8. Results

A normal valve cycle includes four phases: opening, equilibrium, closing and closed [11]. Fig. 5 depicts various valve configurations and streamlines corresponding to each phase.

In the opening phase (Fig. 5a,b), accelerating blood flow led to strong impact on the leaflets. Owing to the studied transvalvular pressure gradient the leaflets turned near the attachment point immediately and made an angle of nearly 25° with normal to the wall. In the equilibrium phase (Fig. 5c), the leaflets slightly oscillated in the opening position. Extended recirculation zone proximal to valve formed in the opening phase and increased in the equilibrium phase. In the closing phase (Fig. 5d), the ejection velocity decreased, the blood flowed reversely. The closing phase ended when the leaflets contacted. In the closed phase (Fig. 5e), the flow pattern varied slightly while leaflets closing became more evident.

The maximum orifice radius, 1.22 mm (25% of the inlet radius), was in the equilibrium phase. This value was consistent with the physiological one (30% of the inlet radius) for the popliteal veins [11]. As shown in Fig. 5c, the outlet maximum velocity was 34 cm/s in equilibrium phase, meanwhile the inlet maximum velocity was 9 cm/s, which complied with the calculated ratio of these velocities (0.33) reported in [2]. Further, the reverse flow in the recirculation zone downstream the valve started at 0.5 s at the outlet and the peak reverse flow velocity appeared in orifice area and was – 4 cm/s (Fig. 5c). It consistent with the findings in [11] that the normal valve can close when the reverse flow velocity was low.

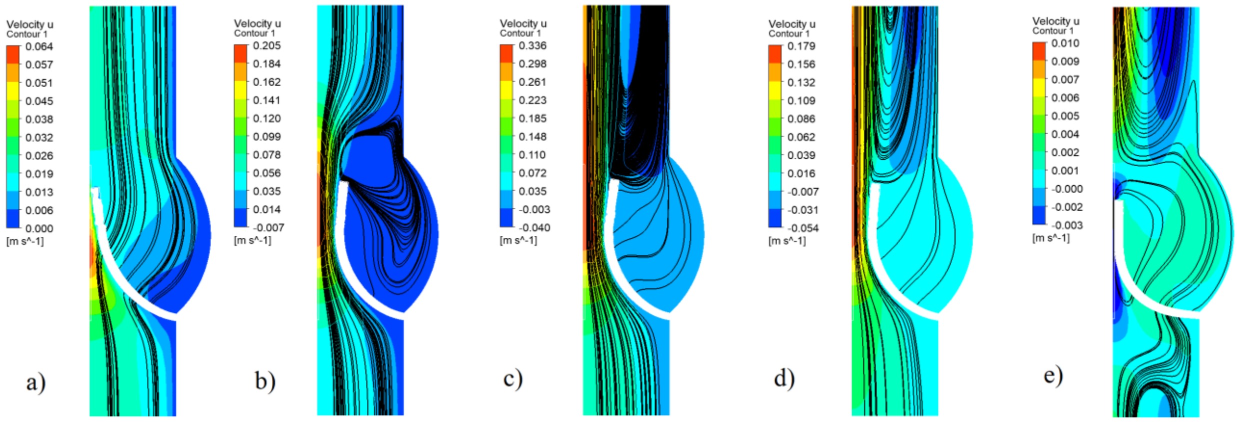

Figure 5. Various valve configurations, axial velocity fields and flow streamlines in a normal venous valve: (a) opening phase, 0.1 s; (b) opening phase, 0.2 s; (c) equilibrium phase, 0.5 s; (d) closing phase, 1 s; (e) closed phase, 1.7 s.

Numerical calculation confirmed that venous valve is closing after extravasal correction with 1/3 diameter narrowing. Consequently correction is successful. The flow structure, e.g. jet and recirculation zones, is more complex versus normal venous valve. Maximum forward and reverse velocities are approximately doubled the values for normal valve (Fig. 6). Maximum orifice valve radius was less than in normal valve – 0.6 mm (12.5% of the initial radius). The contact area was in the vicinity of leaflets tip as opposed to contact area up to a third of the leaflet length for a normal valve.

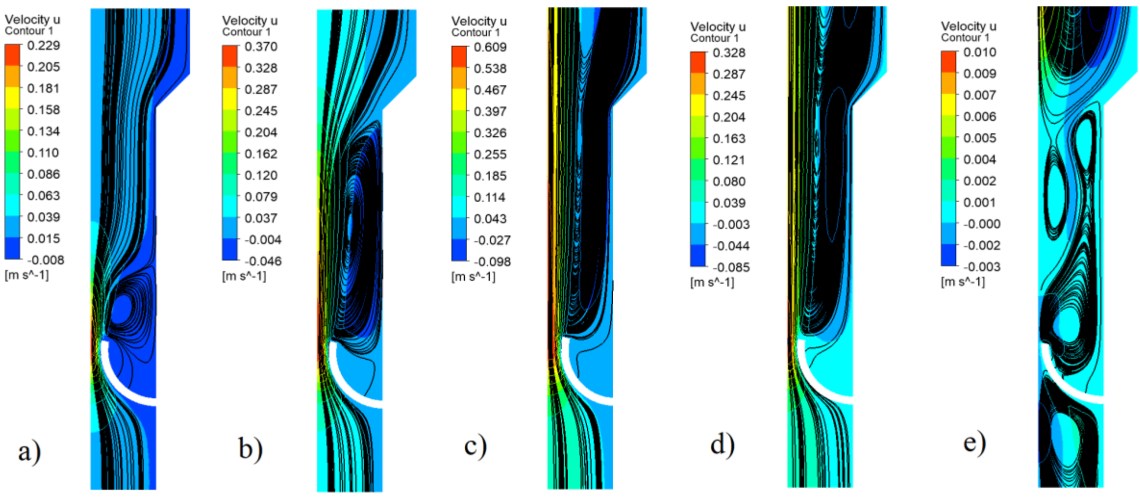

Figure 6. Various valve configurations, axial velocity fields and streamlines in a venous valve after extravasal correction: (a) opening phase, 0.1 s; (b) opening phase, 0.2 s; (c) equilibrium phase, 0.5 s; (d) closing phase, 1 s; (e) closed phase, 1.7 s.

In the stagnant zones fluid moves at a relatively low (velocity less than 1 cm/s) and red blood cells can form agglomerations. Fig. 7 shows stagnant zones in the normal venous valve and venous valve after correction. One stagnant zone is observed behind the normal venous valve. However in the venous valve after correction additionally two new stagnant zones appeared - before and after vein narrowing. These zones are dangerous due to potential thrombosis.

Figure 7. Stagnant zones (grey areas) in a normal venous valve (a) and venous valve after extravasal correction (b) in the opening phase, 0.2 s.

9. Conclusions

The numerical simulation of the popliteal venous valve after extravasal correction showed the hemodynamic efficiency of this reconstructive surgery. Venous valve after extravasal correction with 1/3 diameter narrowing provides complete closure, so it was showed that correction is successful. Besides three stagnant zones instead one in normal venous valve (dangerous due to potential thrombosis) are observed in venous valve after correction. The results obtained can be used by phlebologists when planning surgical interventions.

Acknowledgments

The work was financially supported by the Ministry of Science and Higher Education of the Russian Federation in the framework of the state assignment «Hemodynamic reactions during complex postural effects and arterial and venous thrombosis».

References

[1] Buxton G A, Clarke N. 2007 *J Biol Phys*. **32** 507–521
[2] Soifer E, Weiss D, Marom G and Einav S. 2017 *Med Biol Eng Comput.* **55**(6) 991–9
[3] Simão M, Ferreira J M, Mora-Rodriguez J and Ramos H M 2016 *Med Biol Eng Comput.* **54** 1591–1609
[4] Ariane M, Vigolo D, Brill A, Nash F G B, Barigou M and Alexiadis A. 2018 *Comput Fluids.* **166** 57–63
[5] Chen H Y, Diaz J A, Lurie F, Chambers S D, Kassab G S 2018 *J Vasc Surg Venous Lymphat Disord*. **6** 517–522
[6] Liu X, Liu L 2019 *PLoS One* 14 (3) 0213012
[7] Gataulin Y A, Yukhnev A D and Rosukhovskiy D A 2018 *J. Phys.: Conf. Ser*. **1128** 012009
[8] Gataulin Y A, Yukhnev A D, Smirnov S I and Rosukhovskiy D A 2019 *J. Phys.: Conf. Ser*. **1359**
[9] Tikhomolova L G, Gataulin Y A, Yukhnev A D and Rosukhovskiy D A 2020 *J. Phys.: Conf. Ser*. **1697**
[10] Prokoshkin S D, Chadaev A P, Ryklina E P and Khmelevskaya I Y 2000. In book: Shape Memory Implants 283-300
[11] Lurie F, Kistner R L and Eklof B The mechanism of venous valve closure in normal physiologic conditions. 2002 *J Vasc Surg*. **35** 713–7